https://doi.org/10.46813/2025-155-019

CALCULATING GLOW DISCHARGE PLASMA PARAMETERS IN AN ARGON ATMOSPHERE FOR THE URAGAN-2M STELLARATOR

Yu.P. Martseniuk, Yu.V. Kovtun

National Science Center "Kharkiv Institute of Physics and Technology", Institute of Plasma Physics, Kharkiv, Ukraine

E-mail: martsenyukY@kipt.kharkov.ua

Numerical calculations of the parameters of the glow discharge plasma were carried out on the basis of a global volume-averaged model. The calculations were carried out for argon, and iron, the main component of stainless steel, was assumed as the cathode material. The electron temperature and density, the density of sputtered iron atoms and iron ions, and the density of metastable argon atoms were calculated as a function of pressure and adsorbed power in the discharge. The results of the calculations of the electron temperature and density were compared with the results of previous experiments and are in satisfactory agreement.

PACS: 52.80.-s; 52.80.Hc; 68.49.Sf

INTRODUCTION

Glow discharge is widely used to solve physical and applied problems, and the study of glow discharge plasma has a long history [1]. In controlled fusion research, glow discharge is used for wall conditioning procedure [2]. The wide application of glow discharge for wall conditioning in toroidal vacuum chambers in many modern tokamaks [3-6] and stellarators [7-9] is due to the efficiency of this method of wall conditioning and its technical simplicity. To optimize the wall conditioning procedure, further studies of the glow discharge plasma parameters and their comparison with numerical simulation results are required. When making a 3D model, it is necessary to take into account a large number of elementary processes, the complex geometry of large toroidal devices, as well as the equipment installed inside the vacuum chamber, which cannot always be precisely specified, the characteristics of the different materials used, which is very complex. Therefore, approximate models are used, for example, in [10,11] 2D concentric spherical geometry was used. At estimations of plasma parameters of low-pressure discharges, when particle losses are predominantly due to diffusion, the global volume-averaged models are widely used, for example, in [12-15]. These steady-state and pulsed plasma discharge models [10, 11] are simple but powerful tools for analysis. They require less computation and the simulation results are easily comparable. In [16], a steady-state reflex discharge model based on a volume-averaged (global) model for argon plasma was proposed and analyzed. Further development of this model was continued in [17], where it takes into account the Penning ionization of sputtered cathode atoms and its influence on the balance of charged particles in the plasma.

Since the Uragan-2M stellarator [18] has and uses glow discharge cleaning [8], and studies of argon glow discharge plasma have been carried out [8, 19]. Therefore, it is of interest to carry out simulations of glow discharge based on global volume-averaged models and compare with experimental results. In this work, the global volume-averaged models [17] were modified to take into account the experimental conditions of the experiments with glow discharge on Uragan-2M.

1. GLOBAL (VOLUME-AVERAGED) MODELS GLOW DISCHARGE

Assuming a low temperature, weakly ionized plasma where particle losses are determined by diffusion, the temperature of the electrons [13], can be determined from the formula (1):

$$\frac{\nu_B}{K_{iz}} = \frac{N_0 V}{A_{eff}}, \quad (1)$$

where K_{iz} is the rate constant for the neutral particle ionization, m^3/s; N_0 – neutral particle density m^{-3}; V is the plasma volume, m^3; $\nu_B=(qT_e/M_i)^{1/2}$ is the Bohm velocity, m/s; A_{eff} is the effective area of charged particle losses, $A_{eff}=A_R h_R$, m^2; A_R is the surface area of the torus, m^2; A_R is the radial relations of the plasma density at the plasma boundary to the plasma density in the center, $h_R=h_{R0}=0.8\cdot(4+r/\lambda_i)^{-1/2}$, where λ_i is the mean free path of an ion in the gas, m. Equation (1) can be reduced to the form (2):

$$T = \frac{N_0^2 V^2 K_{iz}^2 M}{A_{eff}^2 q}. \quad (2)$$

The density of electrons is determined from the relation [13] as (3):

$$N_e = \frac{P_{abs}}{q\nu_B A_{eff}\left(E_{iz}+E_e+E_i\right)}, \quad (3)$$

where N_e is the electron density in plasma, m^{-3}; P_{abs} is adsorbed power, W; q is the elementary charge, C; E_{iz} is the average energy required for the formation of an ion-electron pair or the ionization cost; E_e is the average kinetic energy taken away by an electron; E_i is the average kinetic energy taken away by ions, which is equal to the sum of the ion energy before entering the layer and the energy acquired in the layer, $E_i=(T_e/2)+qV_s$, where T_e is the temperature of electrons, eV, V_s is the cathode potential drop, which is approximately equal to the discharge voltage V_{dc}.

The interaction of the plasma with the wall of the vacuum chamber (cathode) causes its sputtered and the entry of the sputtered material into the plasma with further ionization [17]. The balance of neutral atomsarrive into the plasma due to the sputtered of cathodes by gas ions and cathode material ions is written as (4):

$$Y_g N_g^+ A_{eff} \nu_B + Y_m N_m^+ A_{eff} \nu_B^m = \frac{N_m}{\tau_i} V + \frac{N_m}{\tau_D} V \text{ ,} \quad (4)$$

where N_m is the density of neutral atoms of a cathode material, m^{-3}; Y_m and Y_g are the sputtering coefficients of the cathode material by metal and gas ions, respectively; N_g^+ is the density of gas ions, m^{-3}; υ_B^m is the Bohm velocity of metal ions, m/s; τ_i the characteristic time of the sputtered atom ionization, s; $\tau_D=\Lambda/D_m$ is the characteristic diffusion time of a sputtered particle, s; Λ is the characteristic diffusion length, m; D_m the diffusion coefficient of a sputtered atom in the gas, $m^2 \cdot s^{-1}$. The values of the constants for the rate of ionization of a metal atom by electron impact and the rate of charge exchange of a gas ion on a metal atom are taken from [20, 21].

From the balance of neutral atoms, formula 4, and taking into account the characteristic ionization time of the atom sputtered [17], we can find the density of neutral atoms in the cathode material using the following formula (5):

$$N_m = \frac{A_{eff}\left[Y_g N_g^+ \nu_B + N_m^+ \nu_B^m (Y_m - 1)\right]\tau_D}{V} . \quad (5)$$

The density of metal ions is determined from the metal ion balance equation (6) [17]:

$$N_m^+ = \frac{K_{iz} N_m N_e V + K_{CT} N_m N_g^+ V + K_{PI} N_m N_g^m V}{\nu_B^M A_{eff}} , (6)$$

where N_m^+ is the density of metal ions, m^{-3}; K_{CT} – constant of gas ion charge exchange on the neutral metal atom, m^3/s; N_g^m the density of metastable gas atoms, m^{-3}; K_{PI} is the rate constant for the Penning ionization of metal atoms by metastable gas atoms, m^3/s.

The balance of metastable atoms [17] is written in general as (7):

$$\sum_i R_{Gener,i} = \sum_i R_{Loss,i} + \frac{N_g^m}{\tau_D^m} , \quad (7)$$

where $R_{Gener,i}$ and $R_{Loss,i}$ are the rates of metastable gas atom creation and loss, respectively, m^3/s; $\tau_D^m=\Lambda/D_g^m$ is the characteristic diffusion time for a metastable particle, s; and D_g^m is the diffusion coefficient of metastable atoms in the gas, m^2/s. The reaction rates are written down as the product of the reagent densities $N_{r,i}$ and the reaction rate constant K: $R=K\times\prod_i N_{r,i}$.

From the equation of the balance of metastable atoms [17], the density of metastable gas atoms (N_g^m) is defined as (8):

$$N_g^m = (N_g N_e K_{exm} + N_e K_4^m N_g^+)\Big/(N_e K_{izm} + N_e K_{dexm} + \\ + N_e K_1^m + N_g^m K_2^m + N_g K_3^m + N_m K_{PI} + \frac{1}{\tau_{dm}}), \quad (8)$$

where K_{exm} – rate constants of metastable argon formation; K_{izm} – rate constant of metastable argon ionization; K_{dexm} – rate constant of argon de-excitation; K_1^m – K_4^m – rate constants of processes with metastable argon.

The main constants and coefficients, with the processes used in formulas (1)-(6), (8), are shown in Table and Figs. 1–3.

Constants and their processes

№	Process	Rate coef-ficient	Meaning	Cita-tion
1	Ar^m+Fe→Ar+Fe+e	K_{PI}	$2.33 \cdot 10^{-16}$	21
2	Ar^++Fe→Ar+Fe^+	K_{CT}	$13.76 \cdot 10^{-15}$	21
3	e+Ar^m→Ar^*+e	K_1^m	$2 \cdot 10^{-13}$	23
4	Ar^m+Ar^m→Ar+ Ar^++e	K_2^m	$6.4 \cdot 10^{-16}$	23
5	Ar+Ar^m→Ar+Ar	K_3^m	$2.3 \cdot 10^{-21}$	23
6	e+Ar+ →Ar^m+$h\upsilon$	K_4^m	10^{-17}	23
7	Diffusion Ar^m	D_g^m	D_g^m	24
8	Secondary emission	γ	γ	25

In Fig. 1 shows the excitation rate constants of a neutral argon atom (1-9) and the total sum of these constants (10). If we take the total sum of the constants (10) (see Fig. 1), we can see that when the electron temperature increases by a factor of 10, it increases from $1 \cdot 10^{-19}$ to $1.67 \cdot 10^{-14}$ m^3/s, which is an increase of ≈ 5 orders of magnitude.

Fig. 2 shows other process constants for the collision of electrons with an argon atom [22, 23]. The largest constant is that of elastic collisions with the atom (see Fig. 2), which is in the order of ≈ $10^{-14}…10^{-13}$ m^3/s, at temperatures from 1 to 10 eV.

As can be seen from Fig. 3, the sputtering coefficients of gas ions (Y_g) and metal ions (Y_m) increase with increasing electron energy (E) [26, 27], and up to ≈ 500 eV the sputtering coefficients of gas ions is larger than that of metal ions. At higher energies, the value of Y_m is larger than that of Y_g. For example, at 2000 eV the Y_m coefficient is 4.51 atoms/ion and the Y_g coefficient is 3.6 atoms/ion. An increase in energy leads to an increase in the sputtering coefficient, which leads to negative processes, such as the destruction of the cathode material and its subsequent sputtering and entry into the plasma.

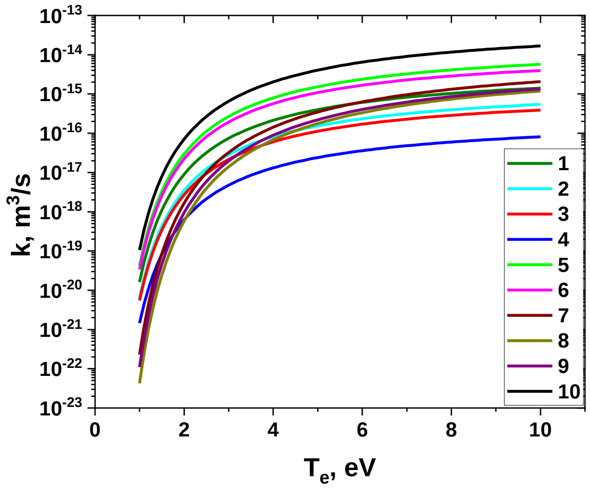

Fig. 1. Dependence of the excitation rate constants of the neutral argon atom (1-9) and their sum (10) on the electron temperature. Excitation of electronic levels: 1 is $^3P_2$; 2 is $^3P_1$; 3 is $^3P_0$; 4 is $^1P_1$; 5 is ^4p; 6 is 4s, 4s′; 7 is 5s, 3d¯, 5s′, 3d′; 8 is 4d, 6s, 4d¯, 4d′, 6s′, 5d, 7s, 5d¯; 9 is highly excited states

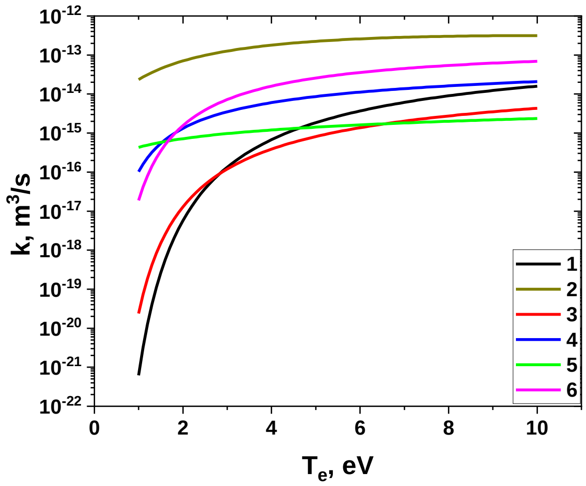

Fig. 2. Dependence of rate constants (1-6) on electron temperature: 1 is the ionization rate constant ($e+Ar \rightarrow Ar^+ +2e$); 2 is the elastic collision rate constant with an atom ($e+Ar \rightarrow Ar+e$); 3 is the rate constant for the formation of metastable argon ($e+Ar \rightarrow Ar^m+e$); 4 is the ionization rate constant for metastable argon ($e+Ar^m \rightarrow Ar+2e$); 5 is the rate constant for the de-excitation of metastable argon ($e+Ar^m \rightarrow Ar+e$); 6 is the rate constant of iron ionization $e+Fe \rightarrow Fe^+ +2e$)

2. RESULTS OF CALCULATION AND DISCUSSION

The initial conditions for the calculations are as follows: major chamber radius R = 1.7 m, minor chamber radius r = 0.34 m; working gas temperature – T_g = 273 K; gas atomic weight A = 39.94 a.u.m.; plasma volume V = 3.879 m^3; plasma torus surface area A_R = 22.819 m^2; cathode material steel (main component iron - Fe).

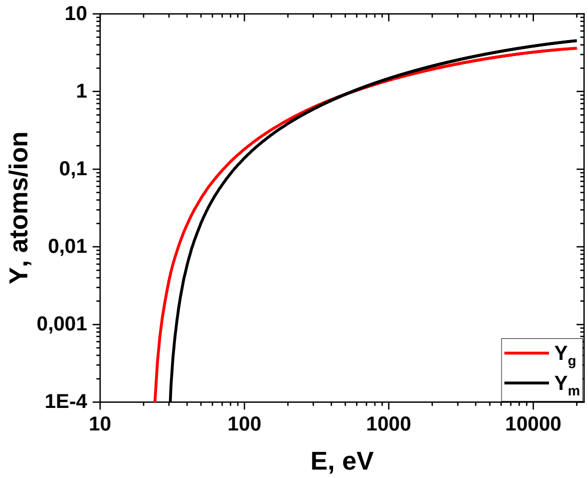

Fig. 3. Dependence of the coefficient of sputtering by gas ions Y_g ($Ar^+ \rightarrow Fe$) and metal ions Y_m ($Fe^+ \rightarrow Fe$) on the ion energy

The results of solving equations 2 and 3, taking into account the experimental conditions, are shown in Figs. 4 to 5. Fig. 4 shows the dependence of the electron temperature on the pressure. As can be seen from Fig. 4, as the argon pressure increases from 0.005 to 20 Pa, the calculated electron temperature decreases from 7.3 to 1.3 eV. An increase in the initial gas pressure, and hence an increase in the concentration of neutral gas atoms, leads to an increase in the probability of electron collisions with gas atoms and energy loss in both elastic and inelastic processes. A similar pattern of dependence, a decrease in electron temperature with an increase in adsorbed power, is observed in [15-17].

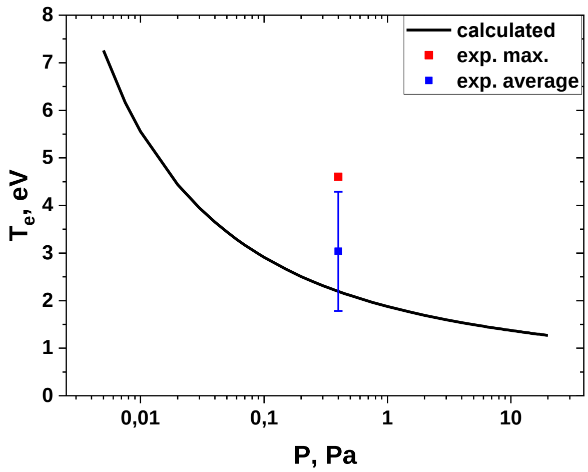

Fig. 4. Dependences of the electron temperature on the pressure: calculated – calculated data, exp. max. and exp. average – maximum and average temperature from the experimental data [19]

Fig. 5 shows the dependence of the electron density on the adsorbed power. An increase of the electron density by ≈ 28.9 times (from $0.5 \cdot 10^{15}$ to $1.2 \cdot 10^{15}$ m^{-3}) is observed with an increase of the adsorbed power by 25 times (from 20 to 500 W). Calculations based on global (volume-averaged) models in [14-17] also showed an increase in electron density with increasing adsorbed power.

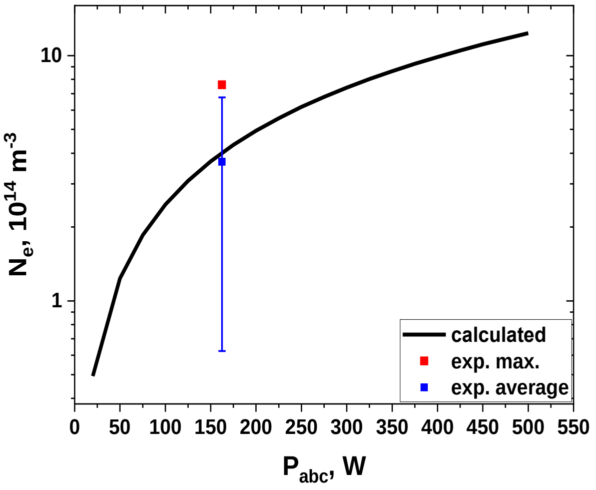

Fig. 5. Dependences of the electron density in plasma on the pressure at P = 0.4 Pa: calculated – calculated data, exp. max. and exp. average – maximum and average densities from experimental data [19]

To compare the calculated results, Figs. 4 and 5 show the experimental results obtained at a working gas pressure of 0.4 Pa and a power of 162.5 W [19]. As can be seen, the calculated data of N_e and T_e are in satisfactory agreement. For example, at P = 0.4 Pa, the average temperature from the experimental data T_e = 3 eV and the calculated T_e = 2.19 eV differ by 27% (see Fig. 4). At P_{abs} = 162.5 W, the average density from the experimental data $N_e = 3.7 \cdot 10^{14}$ m^{-3} and the calculated $N_e = 4 \cdot 10^{14}$ m^{-3} differ by 7.5% (see Fig. 5).

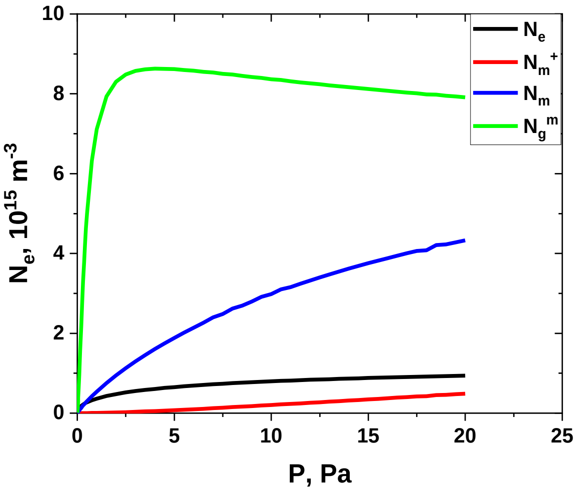

Fig. 6. Dependences of the particle densities in plasma on the pressure at P_{abs} = 100 W: N_e – plasma electrons; N_m^+ – metal ions; N_m – metal atoms; N_g^m – metastable Ar atoms

As a result of solving equations (3), (5), (6), and (8), the density dependence of plasma electrons, neutral metal atoms, gas ions and metastable Ar atoms was obtained and is shown in Figs. 6–9.

Fig. 6 shows the dependence of the density of particles in the plasma on the gas pressure. It can be seen that the density of neutral atoms of the cathode material (N_m) and metal ions (N_m^+) increases with increasing pressure. The density of electrons (N_e), starting from a pressure of ≈ 2.5 Pa, changes slightly with increasing pressure. At the same time, the density of metastable gas atoms (N_g^m) increases up to a pressure of ≈ 2.5 Pa and then decreases with increasing pressure. This may be due to an increase in the number of collisions of metastable atoms with gas and metal atoms, resulting in the loss of metastable atoms.

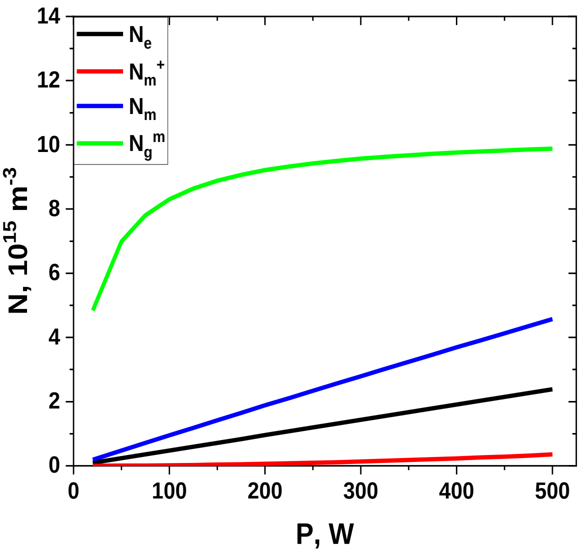

Fig. 7. Dependences of the particle densities in plasma on the adsorbed power in the discharge at P = 2 Pa: N_e – plasma electron;, N_m^+ – metal ions; N_m – metal atoms; N_g^m – metastable Ar atoms

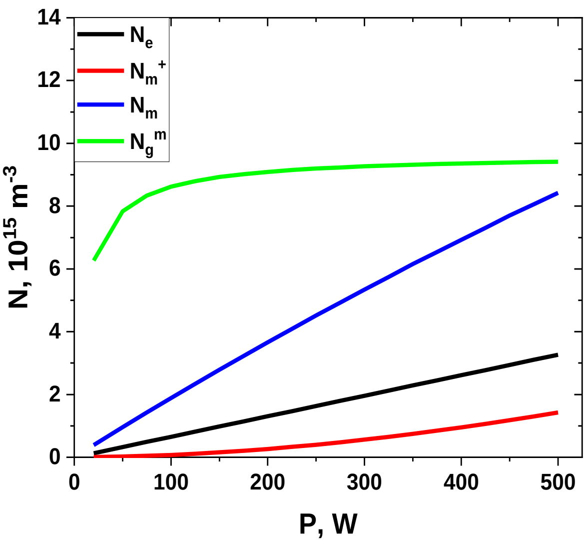

Fig. 8. Dependence of the particle densities in plasma on the adsorbed power in the discharge at P = 5 Pa: N_e – plasma electrons; N_m^+ – metal ions; N_m – metal atoms; N_g^m – metastable Ar atoms

Figs. 7–9 show the dependence of the particle density on the adsorbed power at different initial argon pressures (2, 5, and 10 Pa). It can be seen that as the adsorbed power increases, so does the particle density. For example, in Fig. 7, the density of plasma electrons (N_e) increases from $9.5 \cdot 10^{13}$ to $2.4 \cdot 10^{15}$ m^{-3}, the density of metal ions (N_m^+) from 1…10^{12} to $3.5{\cdot}10^{14}$ m^{-3}, the density of metal atoms (N_m) from $1.9{\cdot}10^{14}$ to $4.5{\cdot}10^{15}$ m^{-3}, the density of metastable Ar atoms (N_g^m) from $4.8{\cdot}10^{15}$ to $9.9{\cdot}10^{15}$ m^{-3}. The density of the particles also increases with increasing pressure (see Figs. 7 and 9), from 2 to 10 Pa. At 500 W, the density values N_e increased by ≈ 1.7 times, N_m^+ by ≈ 9.9 times, N_m by ≈ 4.9 times. The effect of increasing power on the density values is also shown in [17], where the values increase. In Fig. 9 the calculations show that the density of metal atoms exceeds the density of metastable Ar atoms.

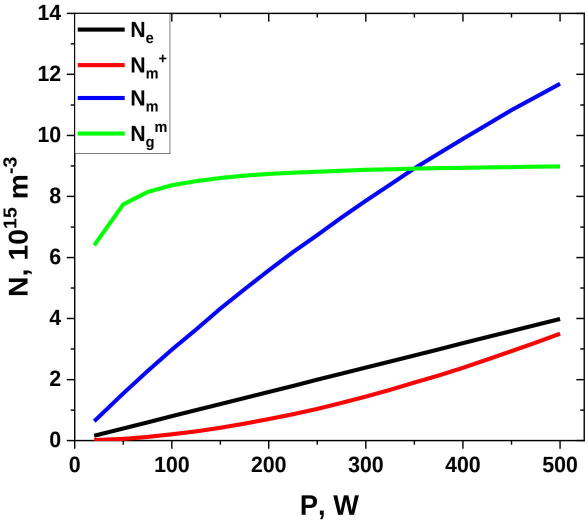

Fig. 9. Dependence of the particle densities in plasma on the adsorbed power in the discharge at P = 10 Pa: N_e – plasma electrons; N_m^+ – metal ions; N_m – metal atoms; N_g^m – metastable Ar atoms

Although this spatially averaged global model is not perfect but simple, since many processes have to be taken into account, it is important to compare the calculations with the experimental data in order to improve the calculations and possibly modify the model.

CONCLUSIONS

Numerical calculations of the parameters of the glow discharge plasma were carried out on the basis of a global averaged model. The calculations were carried out for argon, and iron (the main component of stainless steel) was assumed to be the cathode material in a toroidal geometry. Dependencies of the electron temperature and density, density of sputtered iron atoms and iron ions, density of metastable argon atoms on pressure and adsorbed power in the discharge were calculated. The calculation showed that under these conditions, the electron temperature is at the level of 1.3…7.3 eV, and the plasma density reaches $1.2{\cdot}10^{15}$ m^{-3} at an adsorbed power of 500 W and a working gas pressure of 0.4 Pa. Comparison of the previous results of temperature and electron density from experiments and the results of calculations are in satisfactory agreement. The considered dependence of the particle density in the plasma on the gas pressure and adsorbed power in the discharge showed an increase in particles with increasing gas pressure and adsorbed power.

ACKNOWLEDGEMENTS

This work has been carried out within the framework of the EUROfusion Consortium, funded by the European Union via the Euratom Research and Training Programme (Grant Agreement No 101052200 – EUROfusion). Views and opinions expressed are however those of the author(s) only and do not necessarily reflect those of the European Union or the European Commission. Neither the European Union nor the European Commission can be held responsible for them.

The work is supported by the National Research Foundation of Ukraine under Grant No. 261/0101 “Critical issues for stellarators as fusion machines”, as a result of the “Excellent Science in Ukraine” competition.

This work has been supported in part by the Ministry of Education and Science of Ukraine within the project PH/56–2024.

REFERENCES

1. Y.P. Raizer. *Gas Discharge Physics*. First Edition, Springer-Verlag, Berlin, Heidelberg, 1991.
2. T. Wauters et al. Wall conditioning in fusion devices with superconducting coils // *Plasma Physics and Controlled Fusion*. 2020, v. 62, issue 3, p. 034002.
3. D. Douai et al. Wall conditioning of JET with the ITER-Like Wall // *Journal of Nuclear Materials*. 2013, v. 438, p. S1172.
4. Z. Zhou et al. Design and application of GDC on EAST Tokamak // *Fusion Engineering and Design*. 2011, v. 86, issue 9-11, p. 1599.
5. K.A. Jadeja et al. Novel approach of pulsed-glow discharge wall conditioning in the ADITYA Upgrade tokamak // *Nuclear Fusion*. 2019, v. 59, issue 8, p. 086005.
6. T. Härtl et al. Optimization of the ASDEX Upgrade glow discharge // *Fusion Engineering and Design*. 2017, v. 124, issue 283.
7. A. Goriaev et al. Wall conditioning at the Wendelstein 7-X stellarator operating with a graphite divertor // *Physica Scripta*. 2020, issue T171, p. 014063.
8. Y.V. Kovtun et al. Design and application of glow discharge cleaning at Uragan-2m stellarator // *Problems of Atomic Science and Technology. Series “Plasma Physics” (131)*. 2021, N 1, p. 19-24.
9. K. Nishimura et al. Development of the plasma operational regime in the large helical device by the various wall conditioning methods // *Journal of Nuclear Materials*. 2005, v. 337-339, p. 431-435.
10. G.J.M. Hagelaar et al. Modelling of tokamak glow discharge cleaning I: physical principles // *Plasma Physics and Controlled Fusion*. 2014, v. 57, issue 2, p. 025008.
11. D. Kogut et al. Modelling of tokamak glow discharge cleaning II: comparison with experiment and application to ITER // *Plasma Physics and Controlled Fusion*. 2015, v. 57, issue 2, p. 025009.

12. C. Lee, M.A. Lieberman. Global model of Ar, O_2, Cl_2, and Ar/O_2 high-density plasma discharges // *Journal of Vacuum Science and Technology A*. 1995, v. 13, issue 2, p. 368-380.
13. M.A. Liberman, A.J. Lichtenberg. *Principles of plasma discharges and materials processing*. John Wiley and Sons, INC Publication, 2005.
14. J.T. Gudmundsson et al. On the plasma parameters of a planar inductive oxygen discharge // *Journal of Physics D: Applied Physics*. 2000, v. 33, issue 11, p. 1323-1331.
15. E.G. Thorsteinsson and J.T. Gudmundsson. A global (volume averaged) model of a nitrogen discharge: I. Steady state // *Plasma Sources Science and Technology*. 2009, v. 18, issue 4, p. 045001.
16. Y.V. Kovtun et al. Calculations for parameters of a stationary reflex discharge // *Problems of Atomic Science and Technology. Series "Plasma Physics"*. 2015, №1(21), p. 201-204.
17. Y.V. Kovtun et al. Effect of penning ionization on the balance of charged particles in plasma of a stationary reflex discharge // *Ukrainian Journal of Physics*. 2016, v. 61, issue 8, p. 702-708.
18. Yu.V. Kovtun et al. ICRF plasma production in gas mixtures in the Uragan-2M stellarator // *Fusion Engineering and Design*. 2023, v. 194, p. 113887.
19. Yu.P. Martseniuk et al. Glow discharge cleaning on the Uragan-2M stellarator // *17th Kudowa Summer School "Towards Fusion Energy"*, 3–7 June 2024, Kudowa-Zdrój, Poland: Book of abstract – Insiitute of Plasma Physics and Laser Microfusion, Warsaw, 2024, p. 54.
20. M.A. Lennon et al. Recommended data on the electron impact ionization of atoms and ions: fluorine to nickel // *Journal of Physical and Chemical Reference Data*. 1988, v. 17, issue 3, p. 1285-1363.
21. A. Bogaerts et al. Calculation of rate constants for asymmetric charge transfer, and their effect on relative sensitivity factors in glow discharge mass spectrometry // *Spectrochimica Acta Part B: Atomic Spectroscopy*. 2007, v. 62, issue 4, p. 325-336.
22. J.T. Guðmundsson. *Notes on the electron excitation rate coefficients for argon and oxygen discharge*: Technical Report RH-21-2002, Science Institute, University of Iceland, 2002.
23. B.C. Zheng, D. Meng, H.L. Che, M.K. Lei. On the pressure effect in energetic deposition of Cu thin films by modulated pulsed power magnetron sputtering: A global plasma model and experiments // *Journal of Applied Physics*. 2015, v. 117, №20, p. 203302.
24. A.V. Phelps et al. Use of secondary-electron yields determined from breakdown data in cathode-fall models for Ar // *Plasma Sources Science and Technology*. 1999, v. 8, issue 4, p. B1-B2.
25. B.M. Smirnov. *Excited Atoms.* Moscow: Energoatomizdat, 1982 (in Russian).
26. A. Bogaerts, R. Gijbels. Modeling of metastable argon atoms in a direct-current glow discharge // *Physical Review A*. 1995, v. 52, issue 5, p. 3743-3751.
27. Y. Yamamura, H. Tawara. Energy dependence of ion-induced sputtering yields from monatomic solids at normal incidence // *Atomic Data and Nuclear Data Tables*. 1996, v. 62, p. 149-253.

Article received 28.12.2024
Article accepted 16.01.2025

РОЗРАХУНОК ПАРАМЕТРІВ ПЛАЗМИ ЖЕВРІЮЧОГО РОЗРЯДУ В АТМОСФЕРІ АРГОНУ ДЛЯ СТЕЛАРАТОРА УРАГАН-2М

Ю.П. Марценюк, Ю.В. Ковтун

Проведено числові розрахунки параметрів плазми жевріючого розряду на основі глобально усередненої моделі. Розрахунки були проведені для аргону. В якості матеріалу катода приймалося залізо – основний компонент нержавіючої сталі. Розраховані залежності електронної температури та густини, густини розпилених атомів заліза та іонів заліза, густини метастабільних атомів аргону від тиску та адсорбованої потужності у розряді. Результати розрахунків температури та густини електронів були порівняні з результатами попередніх експериментів та знаходяться у задовільній згоді.